ISSN 1070-3632, Russian Journal of General Chemistry, 2012, Vol. 82, No. 12, pp. 2116–2131. © Pleiades Publishing, Ltd., 2012.
Original Russian Text © Lixin Cheng, 2011, published in Rossiiskii Khimicheskii Zhurnal, 2011, Vol. 55, No. 2, pp. 85–98.

Critical Heat Flux in Microscale Channels and Confined Spaces: A Review on Experimental Studies and Prediction Methods

Lixin Cheng

School of Engineering, University of Aberdeen, King's College, Aberdeen, AB24 3UE, Scotland, UK
e-mail: lixincheng@hotmail.com

Received May 5, 2011

Abstract—This paper presents a comprehensive literature review on critical heat flux (CHF) of flow boiling and pool boiling in micrscale channels and confined spaces. First, distinction between macro- and micro-scale channels is discussed. Then, the critical heat flux mechanisms are discussed. Next, experimental and theoretical studies of subcooled flow boiling CHF in microscale channels together with the prediction methods are reviewed. Following this, experimental and theoretical studies on saturated flow boiling CHF together with the prediction methods are summarized. Furthermore, experimental and theoretical studies on nucleate pool boiling CHF in confined spaces together with the prediction methods are briefly reviewed. So far, limited studies on CHF in microscale channels and confined spaces are available in the literature and there are numerous discrepancies in the existing studies on CHF results and mechanisms. There are no generalized prediction methods for CHF in microscale channels and confined spaces. According to this review, future research needs have been identified, including the frontier research of nanofluids CHF in microscale channels and confined spaces.

DOI: 10.1134/S1070363212120328

INTRODUCTION

Applications of microscale and nanoscale thermal and fluid transport phenomena involved in traditional industries and highly specialized fields, such as bioengineering, micro-fabricated fluidic systems, microelectronics, aerospace technology, micro heat pipes and chips cooling etc., have been becoming especially important over the past years. With the rapid miniaturization of devices to microscale and nanoscale, new technologies taking advantage of these advances are faced with very serious heat dissipation problems per unit volume [1−8]. For example, the thermal management of electronic devices has become challenging due to the continuous and rapid development of integrated circuit technology. With the increased packaging density and performance of microelectronic devices, IC chip power has significantly risen in the last two decades. Current developments in these applications point to the need to dissipate as high as 1000 W cm^{-2} at the device level. This means that the conventional cooling technology, i.e. air cooling, will no longer be able to satisfy these heat duties [6−8]. Thus, it is essential to develop new high heat flux cooling technology to meet the challenging heat dissipation requirements. Flow boiling in micro-channels has become one of the "hottest" research topics in heat transfer as a high efficient cooling technology [6−8] as it has numerous advantages of high heat transfer performance, low pressure drops, chip temperature uniformity and hot spots cooling capability etc. However, gas liquid two-phase flow and flow boiling heat transfer characteristics in microcale channels are quite different from those in macroscale channels. Channel confinement has a great effect the heat transfer and two phase flow characteristics [3, 6, 8]. The available studies focus on boiling incipience, two phase flow patterns, hydrodynamic instability, heat transfer and pressure drop. The issue of critical heat flux (CHF), however, has received very limited attention, despite the great importance of this parameter to the design and safe operation of a heat sink. The ability to predict CHF is therefore of paramount importance to the integrity of the device. Furthermore, nucleate pool boiling CHF in confined spaces have also been studies as pointed out by Cheng et al. [9], which may be related to flow boiling in microscale channels and help

to understand the CHF mechanisms. In recent years, a new research frontier of nanofluids two phase flow and heat transfer is under rapid development [10, 11]. It seems that nanofluids may significantly enhance nucleate pool boiling CHF. Further research is necessary to investigate the CHF of nanofluids in microscale channels and confined spaces. It beyond the scope of this review which focuses on pure fluids but it is essential to mention few words about this new frontier research area here.

The CHF condition sets an upper limit on flow boiling heat transfer in microscale channels. In order to design efficient micron-sized heat transfer devices, it is essential to have a clear understanding of the CHF mechanisms at microscale and to develop reasonable CHF prediction methods. Thus, this study is aiming at providing a literature survey on the experimental and theoretical aspects of CHF, including CHF correlations and models for flow boiling CHF in microcale channels. Both subcooled and saturated flow boiling are concerned. Furthermore, studies on nucleate pool boiling in confined spaces are also briefly reviewed. According to this review, future research needs of CHF in microscale channels and confined spaced have been identified, including nanofluids CHF in microscale channels and confined spaces.

Macroscale to Microscale Criteria

One very important issue should be clarified about the distinction between micro-scale channels and macro-scale channels at first. However, a universal agreement is not yet clearly established in the literature. Instead, there are various definitions on this issue. [3, 5, 10] have summarized different definitions in the literature. Here just show one example, based on engineering practice and application areas such as refrigeration industry in the small tonnage units, compact evaporators employed in automotive, aerospace, air separation and cryogenic industries, cooling elements in the field of microelectronics and micro-electro-mechanical-systems (MEMS), Kandlikar [1] defined the following ranges of hydraulic diameters D_h which are attributed to different channels:

Conventional channels: $D_h > 3$ mm.

Minichannels: $D_h = 200$ μm–3 mm.

Microchannels: $D_h = 10$–200 μm.

According to this definition, the distinction between small and conventional size channels is 3 mm.

The definition of a microscale channel is quite confusing because there are different criteria available as described above. So far, the distinction of microscale channels is not yet established. In this review, the distinction between macro- and micro-scale channels by the threshold diameter of 3 mm is adopted due to the lack of a well-established theory, but is in line with those recommended by Kandlikar [1]. Using this threshold diameter enables more relevant studies to be included.

Critical Heat Flux Phenomena and Mechanisms

Heat transfer coefficient in flow boiling could fall rapidly and the wall temperature increase rapidly at some point along a heated channel. This phenomenon is called the critical heat flux (CHF) and may also be known by many names such as burnout, dryout, DNB and boiling crisis critical heat flux. The CHF is arguably the most important design limit for systems involving heat dissipation from heat-flux controlled surfaces. The occurrence of CHF is associated with a sudden, large reduction in the heat transfer coefficient, which is caused by the loss of liquid contact with the solid surface upon which evaporation or flow boiling (nucleate pool boiling) is occurring. Depending on heat flux magnitude, thermophysical properties, and operating conditions, the loss of coolant contact can result in surface overheating, burnout, or some other form of catastrophic system failure. It is hence of importance for designers to place on accurately determining the CHF limit.

According to whether the bulk fluid at channel outlet is subcooled or saturated when CHF occurs, flow-boiling CHF can be classified as either subcooled CHF or saturated CHF. The two types of CHF are triggered by drastically different mechanisms as shown in Fig. 1 [12].

As shown in Fig. 1a, saturated CHF is encountered in situations where the bulk fluid temperature is larger than saturation temperature at $x_0 > 0$ when CHF occurs. Conditions that commonly lead to saturated CHF include small mass velocity, low inlet subcooling, and/or channels with a large length-to-diameter ratio. The corresponding flow pattern at the channel outlet is mostly annular with the vapor phase occupying most of the channel core while the liquid flows as a thin film along the channel wall. Dryout of the liquid film near the outlet is widely regarded as the trigger mechanism for saturated CHF.

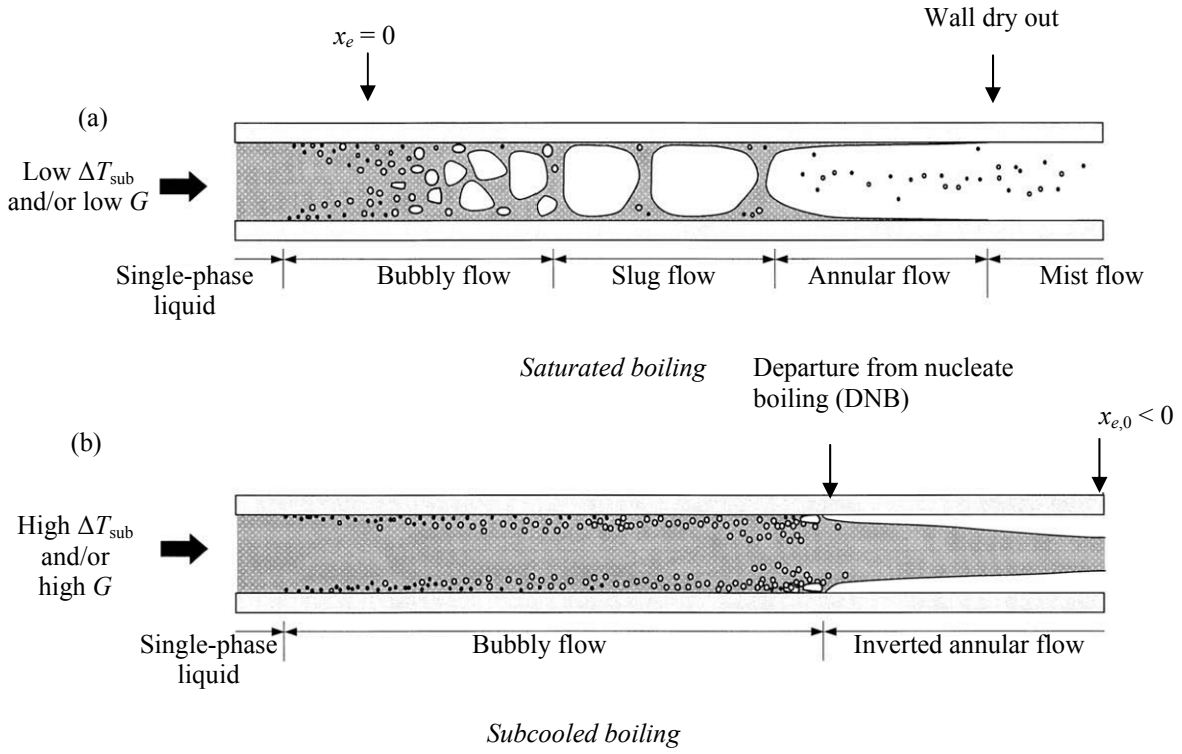

Fig. 1. CHF mechanisms for flow boiling in uniformly heated tubes: (a) dryout in saturated flow boiling and (b) departure of nucleate boiling (DNB) in subcooled flow boiling [12].

As shown in Fig. 1b, subcooled CHF indicates situations where the bulk fluid temperature at the channel outlet is subcooled when CHF occurs. This condition is represented by a thermodynamic equilibrium quality less than zero at the outlet, $x_0 < 0$. Conditions that often lead to subcooled CHF include large mass velocity, high inlet subcooling, and/or channels with a small length-to-diameter ratio. At the channel outlet, the bulk fluid remains in mostly liquid state with a large number of very small vapor bubbles confined to the heated wall. Several theories have been proposed to explain the trigger mechanism for subcooled CHF: intense boiling causes the bubble-liquid boundary layer to be separated from the heated wall and the resulting stagnant liquid to evaporate, bubble crowding within the boundary layer inhibits liquid replenishment near the surface causing the formation of an insulating vapor layer, and dryout of a liquid sublayer beneath large vapor bubbles causes the local wall temperature to rise appreciably.

In the past several decades, the nuclear and conventional power industries have spent enormous resources to investigate CHF for a multitude of pool and flow boiling configurations, mostly in the macroscale range, with some studies in small scale channels. In spite of the large number of articles published to date, an exact theory of CHF has not yet been obtained. As the transport process behind the flow boiling CHF is extremely complex, CHF prediction relies heavily on empirical correlations derived from experimental CHF databases. Traditional flow boiling CHF correlations may not be suitable to predict CHF in microscale channels since the databases from which they were derived may not include enough databases taken from microscale channels and thus the accurate effect of channel dimension on CHF may not be reflected. Furthermore, confinement has a significant on nucleate pool boiling CHF and thus conventional prediction methods normally do not work well for confined space conditions. Therefore, the applicability of existing CHF correlations to microscale channels and confined spaces should be carefully examined in detail.

Although many analytical and experimental studies related to flow boiling CHF in microscale channels and nucleate pool boiling in confined spaces have been

performed for the past years, in the current status of this subject, sufficient, systematic and accurate databases are still unavailable to understand CHF in small- diameter channels and confined spaces, and reliable CHF correlations applicable to a wide range of parameters for microscale channels and confined spaces have not been developed yet. Furthermore, CHF in a heat sink containing multiple parallel channels may be significantly different from that in a single channel, as boiling and two-phase flow is less stable in the former. Various channel shapes such as circular, rectangular channels with different aspect ratios are used and thus should have a significant effect on CHF. Nucleate boiling in different confined space arrangements may exhibit quite different CHF behaviors. Thus, continuous effort to understand the CHF mechanisms and prediction methods in microscale channels and confined spaces are still needed.

Reviews of Studies on Subcooled Flow Boiling Critical Heat Flux

Table 1 summarizes the experimental and theoretical studies on subcooled flow boiling in microscale channels in the literature. Celata et al. [13] investigated CHF in subcooled flow boiling in a 2.5 mm diameter tube and their results showed extremely high critical heat fluxes (reaching values as high as 60 MW m^{-2}). Taking into account a data bank with 500 results,

Table 1. Summary of experimental and theoretical studies on subcooled flow boiling CHF in microscale channels

Author/year/reference	Fluid	Channel diameter/gap, mm	Pressure, bar	Mass flux, kg m^{-2} s^{-1}	Contents
Celata et al., 1993 [13]	Water	Circular, 0.3 to 15	1 to 55	2000 to 40500	Analysis of channel diameter effect on CHF
Celata et al., 1993 [14]	Water	Circular, 2.5	1 to 25	10000 to 40000	Experiments and evaluation of correlations
Celata et al., 1996 [16]	Water	Circular, 0.5 to 32	50	7500	Analysis of diameter effect on CHF
Mudawar and Bowers, 1999 [17]; Hall and Mudawar, 1999 [18]	Water	Circular, 0.406 to 2.54	2.5 to 172.4	5000 to 134,000	Analysis of database and development of correlations.
Hall and Mudawar, 2000 [19, 20]	Water	Circular, 0.25 to 44.7	1 to 200	10 to 134,000	Analysis of database and development of correlations.
Liu et al., 2000 [21]	Water, nitrogen and R113	Circular, 0.3 to 37.5	1 to 192.5	900 to 90,000	Development of a theoretical model
Kureta and Akimoto, 2002 [22]	Water	Rectangular channels with gaps of 0.2 to 3 mm and channel width of 7 to 22 mm	1	846 to15100	Experiments and development of a correlation.
Sarma et al., 2006 [23]	Water	Circular, 0.33 to 3	0.92 to 30	757.9 to 9000	Development of a correlation
Zhang et al., 2007 [24]	FC-72	Rectangular single channel: 5 mm × 2.5 mm	1.38 to 1.52	0.5 to 1.5 m/s	Visualization of CHF phenomena and mechanism
Roday et al. 2008 [25]	Water	Circular, 0.427 mm	1.79, 1.02 and 0.253	315 to 1570	Experiments and analysis
Roday and Jensen, 2009 [26, 27]	Water and R123	Circular, 0.286 to 0.7	0.26 to2.25	320 to 1570	Experiments and development of a correlation
Lee and Mudawar, 2009 [12]	HFE7100	Rectangular multi-channels with hydraulic diameter from 0.1757 to 0.4159	1.1671 to 1.481	670.2 to 2345.5	Experiments and CHF mechanism

Celata et al. [14] analyzed the influence of tube inner diameter on CHF: they have concluded that small channel diameters can lead to very high CHF, especially for high fluid velocities. In [16], the same authors analyzed the diameter effect on subcooled flow boiling CHF and determined a correction factor to their previous model [15] to account for the diameter effect in a wide range of tube diameter from 0.5 to 32 mm.

Mudawar and Bowers [17] performed an experimental study on ultra-high critical heat flux under subcooled water flow boiling for a wide range of tube

Nomenclature

A – cross-sectional area of flow channel, m^2;

A_H – heat transfer area, m^2;

Bi – Biot number defined by Eq. (28);

Bo_{CHF} – Boiling number based on critical heat flux, defined by Eq. (4);

Bo – Bond number defined by Eq. (36);

C_1 – heating geometry parameter 1 defined by Eq. (6);

C_2 – heating geometry parameter 2 defined by Eq. (7);

C^+ – geometry parameter defined by Eq. (10);

c_m – liquid phase specific heat of metal, J kg^{-1} K^{-1};

$c_{p,f}$ – liquid phase specific heat at constant pressure, J kg^{-1} K^{-1};

Co – Confinement number defined by Eq. (26);

D_{eq} – equivalent heated surface diameter, m;

D_h – hydraulic diameter, m;

D – disc diameter, m;

f – friction factor;

G – total vapor and liquid two-phase mass flux, kg m^{-2} s^{-1};

G^* – dimensionless mass velocity defined by Eq. (18);

G – gravitational acceleration, 9.81 m s^{-2};

H – convective heat transfer coefficient, W $m^{-2}K$;

h_{fg} – latent heat of vaporization, J kg^{-1};

k_f – liquid thermal conductivity, W mK^{-1};

k_m – metal thermal conductivity, W mK^{-1};

L_c – characteristic length defined by Eq. (29), m;

L_H – heated length, m;

P_H – heated perimeter, m;

P_W – wetted perimeter, m;

P – pressure, Pa/bar;

q_{CHF} – critical heat flux, W m^{-2};

q_{tot} – heat flux based on total base area of microchannel heat sink, W m^{-2};

Re – Reynolds number considering the total vapor-liquid flow as liquid flow [$GD/(m_L)$];

S – channel gap, m;

T – temperature, °C;

T_{sat} – saturation temperature, °C;

U – mean liquid velocity at inlet to heated section of channel, m s^{-1};

V – volume, m^3;

W – channel width, m;

w_H – width of heated surface, m;

We_D – Weber number defined by Eq. (4);

We_L – Weber number defined by Eq. (23);

x_{crit} – local vapor quality at dryout condition;

x_{ex} – equilibrium vapor quality at the exit of the heated section;

$x_{i,*}$ – pseudo-inlet quality, $(h_i - h_{f,o})/h_{fg,o}$, with saturated thermophyiscal properties evaluated at outlet;

x_i – equilibrium vapor quality at the inlet of the heated section;

x_0 – equilibrium vapor quality at the inlet of the heated section;

$x_{0,CHF}$ – critical quality defined by Eq. (8);

Δh_i – specific enthalpy difference (inlet subcooling), J kg^{-1};

$\Delta T_{sub,0}$ – subcooling at downstream edge of heated section of channel, $T_{sat,0} - T_0$;

Taylor wavelength, m;

μ – dynamic viscosity, Ns m^{-2};

N – kinematic viscosity, m^2 s^{-1};

θ – inclination angle, deg;

ρ_f – liquid density, kg m^{-3};

ρ_g – gas density, kg m^{-3};

ρ_m – metal density, kg m^{-3};

surface tension, N m^{-1};

diameter of 0.406 to 2.54 mm, heated length-to-diameter ratio from 2.4 to 34.1, mass velocity from 5000 to 134000 kg $m^{-2} s^{-1}$, and outlet pressure of 2.5 to 172.4 bars. They studied the parametric trends of CHF relative to all important flow and geometrical parameters. They have found that CHF increased with increasing mass velocity, increasing subcooling, decreasing tube diameter and decreasing heated length-to-diameter ratio. For a constant inlet temperature, CHF increased with increasing pressure up to 30 bars, remained fairly constant between 30 and 150 bars and decreased afterwards as the critical pressure was approached. CHF was accompanied by physical "burnout" of the tube wall near the exit and tube material had little effect on the magnitude of CHF. Hall and Mudawar [18] compiled a high-CHF database for subcooled flow boiling of water in tubes for mass velocity larger than 5000 kg $m^{-2} s^{-1}$ and small diameter tubes (≤ 3 mm). They then developed subcooled high-CHF correlations including two inlet conditions correlations and one outlet conditions correlation. The inlet conditions correlations are based on independent variables (L_H/D_h, x_i) and the outlet conditions correlation is based on dependent variable (x_0). The details of these correlations are not presented here but can be referred to in their paper [18].

The same authors [19, 20] provided a comprehensive review of the current state of knowledge of subcooled CHF for water flow boiling in channels, and derived a statistical correlation based on the entire world subcooled CHF database available until 1999. They compiled a worldwide critical heat flux database with over 30,000 experimental CHF data for boiling of water at subcooled and saturated conditions, including diameter from 0.25 to 44.7 mm and mass velocities from 10 to 134000 kg $m^{-2} s^{-1}$, pressure from 0.7 to 218 bars, inlet subcooling from 0 to 347°C and inlet qualities from –3 to 0. They also compiled all known subcooled CHF correlations for water flowing in a uniformly heated tube and assessed these correlations using their database. They then proposed a new simple, subcooled CHF correlation superior in accuracy to existing correlations which are optimized subcooled CHF correlation based on their previous correlations [18] but with different constants:

The correlation based on outlet conditions [20]:

$$\mathrm{Bo}_{\mathrm{CHF}} = 0.072\mathrm{We}_{\mathrm{D}}^{-0.312}\left(\frac{\rho_f}{\rho_g}\right)^{-0.644}\left[1 - 0.9\left(\frac{\rho_f}{\rho_g}\right)^{0.724} x_0\right]. \quad (1)$$

The correlation based on inlet conditions (recommended) [18]:

$$\mathrm{Bo}_{\mathrm{CHF}} = \frac{0.072\mathrm{We}_{\mathrm{D}}^{-0.312}\left(\frac{\rho_f}{\rho_g}\right)^{-0.644}\left[1 - 0.9\left(\frac{\rho_f}{\rho_g}\right)^{0.724} x_{i,*}\right]}{1 + 0.25992\,\mathrm{We}_{\mathrm{D}}^{-0.312}\left(\frac{\rho_f}{\rho_g}\right)^{-0.08}\left(\frac{L_H}{D_h}\right)}, \quad (2)$$

$$\mathrm{Bo}_{\mathrm{CHF}} = \frac{q_{\mathrm{CHF}}}{h_{\mathrm{fg}}G}, \quad (3)$$

$$\mathrm{We}_D = \frac{G^2 D_h}{\sigma\rho_f}, \quad (4)$$

where x_0 is thermodynamic equilibrium quality, $(h - h_{f,0})/h_{fg,o}$, with saturated thermophysical properties evaluated at outlet pressure, $x_{i,*}$ is pseudo-inlet quality, $(h_i - h_{f,o})/h_{fg,o}$, with saturated thermophysical proerties evaluated at outlet pressure. The critical heat flux q_{CHF} is based on the inside diameter of the channels.

Liu et al. [21] developed a theoretical CHF prediction method for subcooled flow boiling based on liquid sublayer dryout mechanism. The model covers a wide range of parameters including microscale diameters. The model is tested over a large data bank (about 2482 points), which shows a general good accuracy. Parametric trends of the CHF in terms of mass flux, pressure, subcooling, channel diameter and ration of heated length to diameter are considered in their model. The details of the model are not presented here due to too many equations but may be referred to in their paper.

Kureta and Akimoto [22] conducted an experimental study on CHF of subcooled flow boiling of water in narrow rectangular channels with heated from one side with channel gap of 0.2 to 3.0 mm, channel width of 7–22 mm and heated length of 50–200 mm. Based on their experimental data, they proposed a CHF correlation for subcooled flow boiling of water in narrow rectangular channels, which is applicable to narrow rectangular channels and small-diameter tubes with two side heated and fully circumferentially heated tubes. Their correlation is based on the critical quality, dimensionless CHF parameter and heated perimeter ratio:

$$\left(\frac{q_{\mathrm{CHF}}}{Gh_{\mathrm{fg}}}\right)\left(\frac{G\lambda}{\sigma}\right)^{0.5} = C_1(x_{\mathrm{e,CHF}} + C_2), \quad (5)$$

where

$$C_1 = \left[6.9\left(\frac{P_H}{P_W}\right)^2 - 10\left(\frac{P_H}{P_W}\right) + 2\right] \times 10^{-3}, \quad (6)$$

$$C_2 = -0.75\left(\frac{P_H}{P_W}\right)^2 + 0.9\left(\frac{P_H}{P_W}\right) + 0.28, \quad (7)$$

$$x_{0,CHF} = x_i + C^+ Bo_{CHF}, \quad (8)$$

$$C^+ = \frac{P_H L_H}{A} = \frac{w_H L_L}{ws}, \quad (9)$$

$$C^+ = \frac{4L_H}{D_h}. \quad (10)$$

Sarma et al. [23] proposed a CHF correlation for small diameter tubes less than 3 mm, which can also be applied to larger diameter tubes:

$$\frac{q_{CHF} D_h}{\mu h_{fg}^{0.5}} = 0.483 Re^{0.62}\left[\frac{pD_h}{\mu h_{fg}^{0.5}}\right]^{0.17}\left[\frac{D_h}{L_H}\right]^{0.5}. \quad (11)$$

Lee and Mudawar [12] recently studied critical heat flux of subcooled flow boiling in micorchannel heat sinks suing HFE7100 with high-speed video. The high subcooling greatly reduced both bubble departure diameter and void fraction and precluded flow pattern transitions beyond the bubbly regime. Critical heat flux was triggered by vapor blanket formation along the microchannel walls despite the presence of abundant core liquid. Figure 2 shows the typical occurrence of subcooling CHF in microchannels. Prior to CHF, there is significant amount of bubbles near the wall with an abundance of liquid in the core. When CHF occurs, bubbles coalesce into continuous vapor blanket, thermally insulating the microchannel walls from liquid contact. This behavior is consistent with the mechanisms of DNB shown in Fig. 1b. There is a sudden sharp rise in the microchannel base temperature. Furthermore, they have found that CHF increases with increasing mass velocity and subcooling and decreasing hydraulic diameter for a given mass flow rate. Furthermore, a modified correlation is proposed for microchannel heat sinks, including rectangular cross-section, three-sided heating and flow interaction between microchannles as

$$Bo_{CHF} = \frac{q_{CHF}}{Gh_{fg}^{0.5}} = \frac{0.0332 We_D^{-0.235}(\rho_f/\rho_g)^{-0.681}[1 - 0.684(\rho_f/\rho_g)^{0.832} x_{e,i}^*]}{1 + 0.0908 We_D^{-0.235}(\rho_f/\rho_g)^{0.151}(L_H/D_h)}. \quad (12)$$

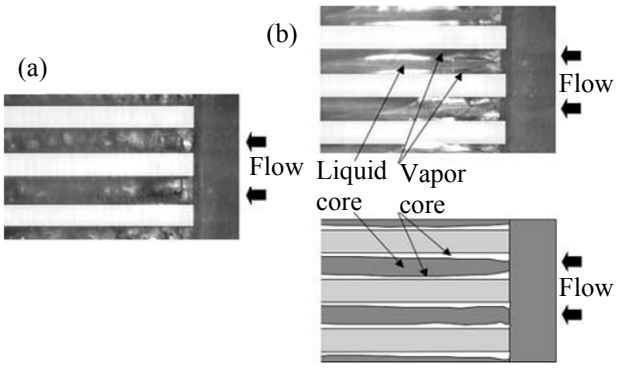

Fig. 2. Flow images for normal DNB with hydraulic diameter D_h = 0.3341 mm at inlet temperature of 0°C and mass velocity of 1341 kg m^{-2} s^{-1} for (a) q_{tot} = 318.3 W cm^{-2} and (b) q_{tot} > 325.8 W cm^{-2} [12].

Zhang et al. [24] studied CHF of highly subcooled conditions using FC-72 for a horizontal channel heated along its bottom wall. High-speed video imaging and photo-micrographic techniques were used to capture interfacial features and reveal the sequence of events leading to CHF. Figure 3 shows their observed CHF process for the indicated conditions, which helps to understand the CHF mechanisms.

Roday et al. [25] performed an experimental study of CHF for a single stainless tube with a diameter of 0.427 mm under uniform heat flux condition. Their experimental results show that the CHF increases with an increase in mass flux and exit pressure. For all exit pressures, the CHF decreased with an increase in quality in the subcooled region, but with further increase with quality (near zero quality and above). Their work also covers saturated flow boiling CHF as in Table 2. Roday and Jensen [26, 27] experimentally studied CHF of flow boiling with water and R123 in single circular channels. They observed the conventional DNB-type behavior in the highly subcooling region, which means the conventional theories are able to explain the CHF of subcooled flow boiling in microchannels, which is inconsistent with other researchers' results [12, 24]. However, for multi-micro channels, this should be further clarified as apparently limited studies are available in the literature, especially, the aspect ratios should have an effect but not explored yet so far. They also proposed a correlation using the dimensionless numbers such Weber number, density ratio, heated length-to-diameter and the enthalpy or inlet quality as

Table 2. Summary of experimental and theoretical studies on saturated flow boiling CHF in microscale channels

Author/year/ reference	Fluid	Channel diameter/gap (mm)	Pressure (bar)/ Saturation temperature (°C)	Mass flux ($kg\ m^{-2}\ s^{-1}$)	Contents
Lazarek and Black, 1982 [30]	R-113	Circular tube, 3.1	1.32 to 4.17	232 to 503	Experiments and development of a correlation for critical vapor quality
Oh and Englert, 1993 [31]	Water	Rectangular channel with a gap width of 1.98 mm	0.2 to 0.95	30 to 80	Experiments and development of correlations
Bowers and Mudawar, 1994 [32]	R-113	Circular tubes, 2.45 and 0.51		Maximum: 95 ml min^{-1}	Experiments and development of a correlation
Roach et al., 1998	Water	Circular, 1.17 and 1.45; micro-rod bundle with a triangular array hydraulic diameter: 1.131	4.07 to12.04	250-1000	Experiments and analysis
Jiang et al., 1999 [33]	Water	V-grooved, hydraulic diameter: 0.04 and 0.08	0.5 to 3.2	Not mentioned	Experiments and analysis
Yu et al., 2002 [51]	Water	Circular, 2.98	2	50 to 200	Experiments and analysis
Qu and Mudawar, 2004 [34]	Water	Rectangular, 21 parallel channels, 0.215 × 0.821	1.213 to1.398	86-368	Experiments and development of a new correlation
Kosar et al., 2005	Water	Rectangular, 5 parallel channels, hydraulic diameter: 0.223	Not mentioned	41-302	Experiments and development of a correlation
Bergles and Kandlikar, 2005 [28]		microchannels			Review of CHF in microchannels
Zhang et al., 2006 [36]	Water	Hydraulic diameter: 0.33–6.22 mm	1 to190	5.33 to 134000	Analysis of the database and development of a correlation
Kosar and Peles, 2007 [40]	R123	Rectangular, 5 parallel channels: 0.2×0.264 mm	2.27 to 5.2	291 to 1118	Experiments and development of a correlation
Qi et al., 2007 [37]	Nitrogen	Circular, 0.531, 0.834, 1.042, and 1.931	0.2, 0.3, 0.5	14 to 44	Experiments and development of a correlation
Agostini et al. 2008 [44]	R236fa	Rectangular, 67 parallel channels, 0.223×0.68	2.032 to 3.427	276 to 992	Experiments and analysis
Wright et al., 2008 [38]	Water	Rectangular, multiple-channel 1×1.27	0.898 to 1.15	9.5 to 39	Experiments an development of a correlation
Tanaka et al., 2009 [39]	Water	Rectangular thin channels with gaps of 1 to 2.4	1	0 to 4000	Analysis of database and development of a correlation
Wojtan et al. 2006 [35]	R134a and R245fa	Circular, 2.46	Exit saturation temperatures: 30 and 35°C	400 to 1600	Experiments and development of a correlation
Roday et al. 2008 [35]	Water	Circular, 0.427	1.79, 1.02 and 0.253	315 to 1570	Experiments and analysis
Roday and Jensen, 2009 [26, 27]	Water and R123	Circular, 0.286 to 0.7	3.5, 4.5, 7, 10.5	315 to 1570	Experiments and analysis
Revellin and Thome, 2008 [43]	R113, R134a, R245fa and water	Circular, 0.509 to 3.15; rectangular, 0.215×0.821	Saturation temperatures: 30 to 109.2°C	29 to 1600	Development of a theoretical model

Table 2. (Contd.)

Author/year/ reference	Fluid	Channel diameter/gap (mm)	Pressure (bar)/ Saturation temperature (°C)	Mass flux (kg m^{-2} s^{-1})	Contents
Kuan and Kandlikar, 2008 [61]	R123 and water	Rectangular, 6 parallel channels: 1.054 × 0.157	0.106 to 2.483	50 to 533.8	Experiments and development of a model
Kuo and Peles, 2008 [41]	Water	Rectangular, parallel channels, hydraulic diameter: 0.227	0.1 to 1	86 to 303	Experiments and development of a correlation
Wu et al., 2009 [42]	Water	Narrow channels with annular gaps of 0.95 and 1.5	6 to 42	60 to 130	Experiments and development of a correlation
Kosar, 2009 [47]	Water, R-123, R-113, R-134a and R-245fa	Circular, and rectangular, single and multiple parallel channels with hydraulic diameters of 0.233 to 3.1	1.01 to 8.88	50 to 1600	Development of a new model
Mauro et al. 2010 [46]	R134a, R236fa and R245fa	Rectangular, 29 parallel channels: 0.199 × 0.756	Saturation temperatures: 20 to 50° C	250–1500	Experiments and analysis
Park and Thome 2010 [45]	R134a, R236fa and R245fa)	Rectangular, 20 parallel channels: 0.467 × 4.052, and 29 parallel channels with 0.199 × 0.756	Saturation temperatures: 10 to 50°C	100–4000	Experiments and analysis

$$\mathrm{Bo}_{\mathrm{CHF}} = \frac{44587\mathrm{We}_{\mathrm{D}}^{1.136}(\rho_{\mathrm{f}}/\rho_{\mathrm{g}})^{-0.625}(L_{\mathrm{H}}/D_{\mathrm{h}})^{-1.68}[(\Delta h_i/h_{\mathrm{fg}}) - 0.0157]}{(\mathrm{We}_{\mathrm{D}} - 0.425)[(L_{\mathrm{H}}/D_{\mathrm{h}}) - 279.8]}. \quad (13)$$

Apparently, there are limited studies on subcooling CHF in microchannels so far. Several correlations have been developed by the researchers according to their own data. Due to the different test condictions and channel geometries, it is difficult to say if these correlations can be extended to other conditions. No generalized correlation is available for subcooling CHF in microchannels so far. Therefore, efforts should be made to obtain systematic experimental data for subcooling CHF under a wide range of test conditions

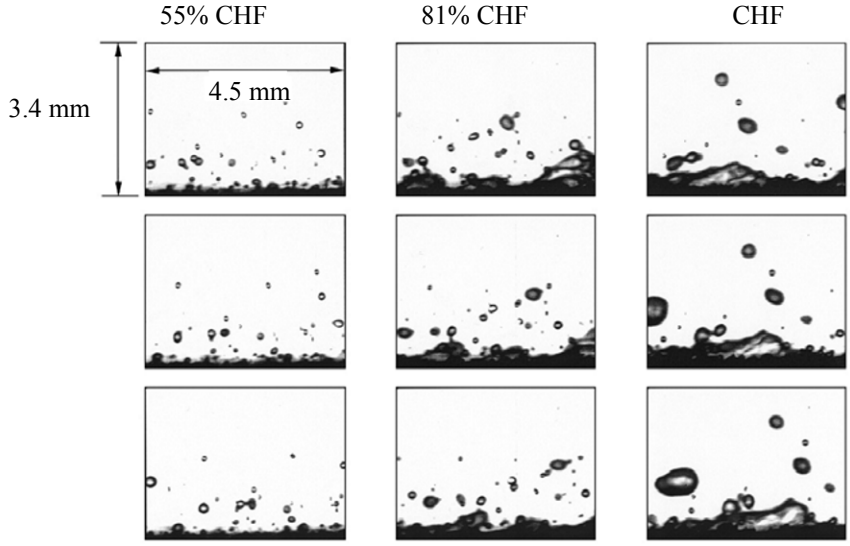

Fig. 3. Magnified sequential images of vapor layer at different heat fluxes leading to CHF for U = 1.2 m s^{-1} and $\Delta T_{\mathrm{sub},\,0}$ = 30°C [24].

and to understanding the physical mechanisms and to develop generalized correlations.

Studies on Saturated Flow Boiling Critical Heat Flux

Table 2 summarizes the experimental and theoretical studies on CHF of saturated flow boiling in microscale channels. These include various conditions such as circular channels, rectangular channels, V-channels for different conditions and fluids. The available experimental studies include the onset of CHF, parametric effects on CHF, critical vapor quality, etc. In general, CHF increases with increasing mass velocity. It also depends on pressure, channel sizes etc. The theoretical studies include evaluation of the available correlations, understanding the CHF mechanisms, instability effects and conjugate heat transfer effects and development of new correlations and models. For example, dryout is the leading mechanisms for CHF, which is the same as for macroscale channels.

Bergles and Kandlikar [28] reviewed the existing studies on critical heat flux in microchannels and found that no CHF data were available for microchannels. For the case of parallel multichannels, they noted that all the available CHF data were taken under unstable conditions. The critical condition is the result of upstream compressible volume instability or the parallel channel, Ledinegg instability. As a result, the CHF values are lower than they would be if the channel flow were kept stable by an inlet restriction at the inlet of each channel. One of the most widely used correlations developed for saturated CHF in single macrotubes is that of Katto and Ohno [29], which has been extended with minor modifications to the microscale channels with limited success so far.

Lazarek and Black [30] conducted an experimental study of saturated flow boiling of R-113 in a round tube with an internal diameter of 3.1 mm and proposed a new critical vapor quality correlation, applicable to low reduced pressure conditions, for predicting the vapor quality at dryout (CHF conditions) in terms of mass velocity, inlet subcooling, and heated length as:

$$x_{\text{crit}} = 1 - 6.075\times10^{-3} G D_{\text{h}}^{0.25} (D_{\text{h}}/L_{\text{H}})^{0.59} [1 + 3.11(\Delta h_i/h_{\text{fg}})]. \quad (14)$$

The correlation predicted their data well.

Oh and Englert [31] conducted an experimental study of CHF for low flow boiling of mass velocity from 30 to 8 kg $m^{-2} s^{-1}$ in vertical uniformly heated thin rectangular channels to simulate natural convection boiling. The aluminium channel was heated on one side and the other side of the channel was a Pyrex window allowing visual observation of the CHF event. New CHF correlations were proposed for both upward and downward flows as:

For downward flow:

$$(A_{\text{H}}/A) q^*_{\text{CHF}} = 0.406 [1 + (\Delta h_i/h_{\text{fg}})] G^* + 2.412. \quad (15)$$

For upward flow:

$$(A_{\text{H}}/A) q^*_{\text{CHF}} = 0.458 [1 + (\Delta h_i/h_{\text{fg}})] G^* + 2.412, \quad (16)$$

$$q^*_{\text{CHF}} = \frac{q_{\text{CHF}}}{h_{fg}\sqrt{\lambda\rho_g g(\rho_f - \rho_g)}}, \quad (17)$$

$$G^* = G/\sqrt{\lambda\rho_g g(\rho_f - \rho_g)}, \quad (18)$$

$$\lambda = \sqrt{\sigma/g(\rho_f - \rho_g)}. \quad (19)$$

One of the earliest studies on CHF in multi-microchannels was carried out by Bowers and Mudawar [32]. They tested a cooling element with an array of 17 circular channels, 0.51 mm diameter, 28.6 mm long, in a 1.59 mm-thick nickel block, heated over the central 10 mm. Boiling curves were generated that terminated in well-defined CHF conditions. CHF was found to be independent of inlet liquid subcooling and almost directly proportional to mass velocity, and a dimensionless correlation was proposed as

$$\frac{q_{\text{CHF}}}{Gh_{\text{fg}}} = 0.16 \text{We}_{\text{D}}^{0.121} (L_{\text{H}}/D_{\text{h}})^{-0.54}, \quad (20)$$

where q_{CHF} is based on the heated channel inside area.

Jiang et al. [33] developed a microchannel heat sink integrated with a heater and an array of implanted temperature sensors. There were 58 or 34 channels of rhombic shape, having a hydraulic diameter of 40 or 80 μm, respectively, in their 10×20 mm^2 test section. CHF data were taken for once–through water entering at 20°C. It appears that the CHF conditions were characterized by the rapid rise in the average of all temperature sensors. The critical power was found to be proportional to the total volumetric flow rate.

Qu and Mudawar [34] performed experimental study of CHF in rectangular multi-microchannels. Their heated block contained 21 channels of 215×821 $μm^2$ size. For their test setup, vapor backflow and

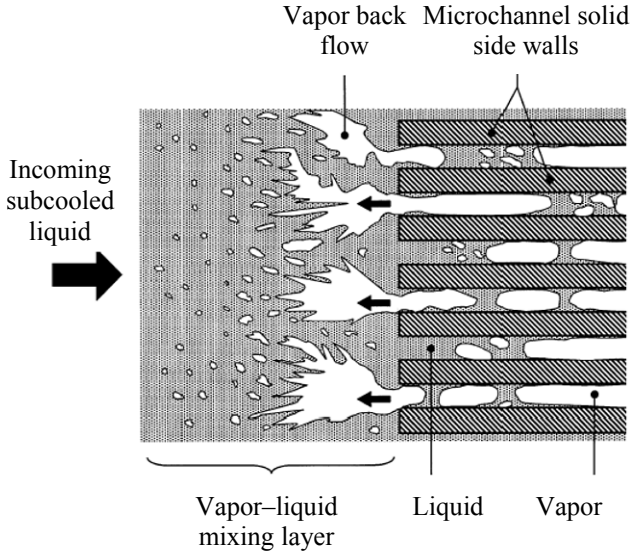

Fig. 4. Schematic representation of observed vapor back-flow as heat flux approaches CHF [34].

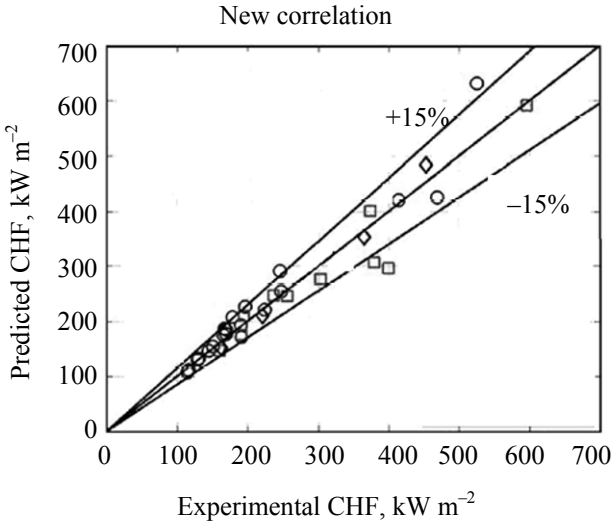

Fig. 5. Comparison of the experimental results to the new correlation [35]. (○) R-134a, 0.5 mm; (□) R-134a, 0.8 mm; (◊) R-245fa, 0.5 mm.

instability from all of the channels into the inlet plenum was observed as CHF was approached. Figure 4 shows the schematic of the micro-channels inlet at these high pre-CHF heat fluxes. Vapor was observed to flow backwards from the individual microchannnels into the upstream shallow plenum, eventually forming a thick intermittent vapor layer. This layer was broken up into many small bubbles, which propagated further upstream even into deep plenum, where it mixed with the incoming liquid. The upstream plenum interactions between the vapor and incoming liquid significantly altered the fluid temperature in the deep plenum. They proposed an extension of the Katto and Ohno [29] correlation for multi-microchannels according to water and R113 test data as

$$q_{CHF} = 33.43\,We_L^{-0.21}(L_H/D_h)^{-0.36}. \quad (21)$$

Wojtan et al. [35] performed limited series of tests on CHF in microchannels to determine the critical heat flux in single 0.5 mm and 0.8 mm internal diameter microchannel tubes as a function of refrigerant mass velocity, heated length, saturation temperature and inlet liquid subcooling. The refrigerants tested were R-134a and R-245fa. The results showed a strong dependence of CHF on mass velocity, heated length and microchannel diameter but no influence of their small liquid subcoolings. Neither the CHF single-channel correlation of Katto and Ohno [29] nor the multichannel correlation of Qu and Mudawar [34] were able to predict their data. Based on their experimental data, a new microscale version of the Katto and Ohno correlation was proposed by Wojtan et al. [35] as

$$q_{CHF} = 0.437\,(\rho_g/\rho_f)^{0.073}We_L^{-0.24}(L_H/D_h)^{-0.72}Gh_{fg}, \quad (22)$$

$$We_L = \frac{G^2 L_H}{\sigma\rho_f}. \quad (23)$$

Their method predicts their experimental data well as shown in Fig. 5. However, no one method was able to predict the total database of these three groups.

Zhang et al. [35] proposed a simple, non-dimensional, inlet conditions dependent CHF correlation for saturated flow boiling, covering diameters from 0.33 to 6.22 mm and wide conditions as

$$Bo_{CHF} = 0.0352[We_D + 0.0119(L_H/D_h)^{2.31}(\rho_g/\rho_f)^{0.361}]^{-0.295} \times (L_H/D_h)^{-0.311}[2.05(\rho_g/\rho_f)^{0.17} - x_i]. \quad (24)$$

Their correlation is among the best of all the tested correlations in their study. But further examination of the correlation is necessary for a wider range of test conditions.

Qi et al. [37] conducted experimental study of CHF of nitrogen saturation flow boiling in micro-circular tubes with diameter of 0.531, 0.834, 1.042, and 1.931 mm. They have found that both the CHF and the critical vapor quality are higher than those for conventional channels. They postulated the mechanisms of CHF in

Table 3. Summary of experimental studies on confined nucleate pool boiling CHF

Author/year/reference	Fluid	Heating space/dimensions (mm)	Pressure (bar)	Remarks
Katto and Kosho, 1979 [52]	Water, R-113, ethyl alcohol and benzene	Disk diameter d = 10 and 20 And the distance between the parallel disks s in a range of d/s = 0–120.	1	Experiments and development of a correlation
Monde et al., 1982 [53]	Water, ethanol, R-113 and benzene	Vertical rectangular channel with gap sizes s = 0.45 to 7 mm and L_H/s <120	1	Experiments and development of a correlation
Fujita et al., 1988 [54]	Water	Confined space with a heating surface width of 30 mm, lengths of 30 and 120 mm and gap sizes of 5, 2, 0.6 and 0.15 mm	1	Experiments, analysis and development of a correlation
Chyu, 1988 [56]	Water, R-113 and acetone	Confined annular crevice with gap sizes from 0.076 to 2.58	1	Development of a prediction method
Kim et al., 2002 [55]	Water	Annuli with gap sizes of 0.5 to 3.5 mm and inclination angles from horizontal to vertical positions.	1	Experiments and development of a new model
Kim and Suh, 2003 [57]	Water	Narrow gap channel with gap sizes of 1, 2, 5 and 10 mm and the sutface orientation angles from the downward-facing position (180°) to vertical position (90°).	1	Experiments and development of a correlation
Geisler and Bar-Cohen, 2009 [59]	FC-72	Vertical, rectangular parallel-plate channels	1	CHF in narrow vertical channels was measured and compared to correlation.
Misale, 2009 [58]	HFE7100	Narrow spaces with gap sizes of 0.5, 1, 2, 3.5, 5 10 and 20 mm. the surface orientations were 0 (horizontal upward surface), 45, 90 and 135.	1	Experiments, analysis and development of a correlation

microtube is the dryout or tear of the thin liquid film near the wall and CHF increases gradually with decrease of the tube diameter. They proposed the following correlation for nitrogen based on the Katto correlation as

$$q_{CHF} = [0.214 + 0.14\mathrm{Co}\,(\rho_g/\rho_f)^{0.133} \times \mathrm{We}_D^{-0.333} \frac{1}{1 + 0.33(L_H/D_h)}, \quad (25)$$

$$\mathrm{Co} = \left[\frac{\sigma}{(\rho_f - \rho_g) g D_h^2} \right]. \quad (26)$$

Wright et al. [38] performed a study on CHF of vertical up-flow of water through multiple thin rectangular channel for low mass flexes of 9.5 to 39 kg m^{-2} s^{-1}, incorporating the conjugate heat transfer effects captured in the Biot number and the ratio of fluid and heated substrate thermal products. Based on their measurement, they proposed the following CHF correlation as

$$(A_H/A) q^*_{CHF} = 3.9 \left(\frac{k_f \rho_f c_{p,f}}{k_m \rho_m c_{p,m}} \right)^{0.5} \left[1 + \left(\frac{\rho_f}{\rho_g} \right)^{0.1} \right]^{-6.7} \times \mathrm{We}_D^{-0.33} \mathrm{Bi} \left[1 + \frac{\Delta h_i}{h_{fg}} \right] G^* + 0.018, \quad (27)$$

$$\mathrm{Bi} = h L_c / k_m, \quad (28)$$

$$L_c = \sqrt{\frac{V}{s}}, \quad (29)$$

$$h = 6.4 \times 10^6 (\mathrm{Bo}^{2.1} \mathrm{We}_D) 0.28 \left(\frac{\rho_g}{\rho_f} \right)^{0.21}. \quad (30)$$

Tanaka et al. [39] recently studied the effect of heated length on critical heat flux in thin rectangular channels under atmospheric pressure. They compared the data for thin rectangular channels with the previous correlations and found that none of these correlations successfully reproduced the data for a wide range of

heated lengths. They proposed a new CHF correlation for a wide range of heated lengths as

$$q^*_{CHF} = \frac{0.5041A\sqrt{D_h/\lambda}}{A_H[1 + (\rho_g \rho_f)^{1/4}]^2} + 0.0047G^*(L/D_h)^{-0.31}, \quad (31)$$

where q_{CHF}^*, G^* and λ are evaluated with Eqs. (17), (18), and (19), respectively.

Kosar and Peles [40] performed an experimental study on CHF of R-123 in silicon-based rectangular multi-microchannels. They also performed flow visualization at CHF condition and concluded that dryout is the leading CHF mechanism. They proposed a new correlation to represent the effect of mass velocity, exit vapor quality and system pressure, which can be found in their paper. Kuo and Peles [41] performed an experimental study on CHF of water in silicon based rectangular multi-microchannels at sub atmospheric pressures. The similar CHF mechanism to the study on R-123 [40] was observed. But they found that the boiling number at the CHF conditions was approximately a constant.

Wu et al. [42] performed an experimental study on critical heat flux of water flow boiling in bilaterally heated narrow vertical annuli with gap sizes of 0.95 and 1.5 mm under a wide range of pressures from 0.6 to 4.2 MPa and very low mass flow velocities from 60 to 130 kg m^{-2}. They also proposed empirical CHF correlations according to their data. However, as these correlations contain heat flux parameters which should be the same values for the CHF if the CHF condition is achieved, it is difficult to understand how to apply these correlations to calculate CHF values.

Some theoretical models for the prediction of the critical heat flux in microhcannels have been developed. Revellin and Thome [43] proposed such a model which is based on the two-phase conservation equations, including the effect of the height of the interfacial waves of annular film. The model contains a non-linear system of five differential equations. Validation of their model with a database from two different laboratories has shown that the model predicts the database well. Agostini et al. [44] compared their measured CHF data to a number of models and correlations and found that the correlation of Wojtan et al. [35] and model of Revellin and Thome [43] are among the best ones. Recently, Park and Thome [45] and Mauro et al. [46] compared their measure data to the model and have confirmed the validation of the model. However, more extensive data should be compared to further validate the model. Kosar [47] proposed a new model to predict saturated CHF in minichannels and microchannels. They applied mass and energy balances to spray annular flow, assuming that the liquid layer completely evaporates at the exit, to obtain a number of equations. Then, critical heat flux and critical exit quality may be obtained by solving these equations using iterative methods. In order to do so, the deposition mass transfer coefficient of Patankar and Puranik [48] should be used. However, it should be realized that the assumption of CHF occurring at the channel exit is not always true. The deposition mass transfer coefficient must be further verified for other fluids and channels including non-circular channels.

There are many disagreements among the available studies on CHF. Roach et al. [49] and Qi et al. [37] found the CHF to increase with increasing channel diameter, but Bergles et al. [50] found an inverse dependence of diameter on CHF. Oh and Englert [31] found a weak linear relationship between inlet subcooling and CHF, but Bowers and Mudawar [32] found that the CHF was not at all affected by the inlet subcooling during their studies in parallel microchannels. Wojtan et al. [35] also found, in their studies with single tubes, that the CHF was not dependent on inlet subcooling. The data by Yu et al. [51] indicated that the CHF increased with an increase in exit quality, but the Wojtan et al. [35] data depict the opposite effect. The CHF studies by Roach et al. [49] shows that the CHF increases with increasing pressure, but the data in some studies do not show a strong dependence of pressure on CHF. Furthermore, many researchers have attempted to predict their data with existing correlations, but with mixed results. Many different correlations have been developed by various researchers based only on their own data, but they are mostly applicable to the limited data range over which the experiments were conducted. Conjugate heat transfer effects have generally been neglected, and the effect of flow instabilities have not been investigated properly during some of the experiments. The effects of axial conduction through the tube walls or through the blocks on which the channels are machined can significantly alter the CHF condition. Most of the experiments have ignored this aspect. Flow oscillations can have a significant negative effect on the CHF condition. Generally, flow distribution in parallel channels tends to be non-

uniform. Since the CHF condition is dependent on flow rate, most of the data from the experiments using parallel channels are not reliable as the flow rate through the individual channels is not exactly known. According to this review, the current literature on CHF in microchannels is not sufficient to predict the boiling crisis over the range of parameters typically encountered in applications. Therefore, there is a clear lack of accurate and validated generalized models to predict CHF in microscale channels.

Studies on Confined Nucleate Pool Boiling Critical Heat Flow

Not many studies on confined nucleate pool boiling CHF are available in the literature, but they may provide some basic understanding of the CHF phenomena. The fundamental mechanisms of confined nucleate pool boiling CHF might also be related to flow boiling in microscale and confined channels somehow although currently no such study which connect confined nucleate pool boiling to flow boiling in microscale channel. Thus, it is worth to briefly summarize such studies here. Table 3 summarizes the experimental and theoretical studies on confined nucleate pool boiling CHF.

Katto and Kosho [52] studied pool boiling CHF in horizontal confined geometries (0°) using water, R-113, ethyl alcohol and benzene and proposed the following correlation

$$q_{CHF} = \rho_g h_{fg}(\rho_f - \rho_g)^{0.25} \times \frac{0.18}{1 + 0.00918(\rho_g/\rho_f)^{0.14}\left[g\dfrac{(\rho_f - \rho_g)d^2}{\sigma}\right]^{0.5}(d/s)}. \quad (32)$$

Monde [53] proposed the following correlation for vertical rectangular confiend channel (90) for water ethanol R-113 and benzene at atmospheric pressure:

$$\frac{q_{CHF}}{\left[\sigma_g(\rho_f - \rho_g)/\rho_g^2\right]^{0.25}} = \frac{0.16}{1 + 6.7\times10^{-4}(\rho_f/\rho_g)^{0.6}(L_H/s)}. \quad (33)$$

Fujita et al. [54] performed experimental studies on pool boiling CHF in confined narrow space with saturated water at atmospheric pressure between heated and unheated parallel rectangular plates. On heating surface with a width of 30 mm, lengths of 30 and 120 mm and gas sizes of 5, 2, 0.6, and 0.15 mm. the mechanisms are analyzed.

Kim et al. [55] performed an experimental study of CHF in narrow gaps at atmospheric conditions of saturated water with outer diameter of inner tube of 19 mm, heated length of 200 mm, annular gas sizes of 0.5 to 3.5 mm and inclination angles from horizontal to vertical positions. They have found that the CHF increases with the gap size and the inclination angle. They proposed one-dimensional model by modifying the friction factor of the Chyu [56] model as:

$$q_{CHF} = \rho_f h_{fg}\left(\frac{s}{L_H}\right)\left[\frac{gL_H\sin\theta(\rho_f/\rho_g - 2)}{1 + fL_H/2s}\right]^{0.5}, \quad (34)$$

$$f = 0.13\left(\frac{\rho_f - \rho_g}{\rho_g}\right)^{0.5}\mathrm{Bo}^{1.3}, \quad (35)$$

$$\mathrm{Bo} = s\left[g\frac{\rho_f - \rho_g}{\sigma}\right]^{0.5}, \quad (36)$$

$$f = 0.041s^{(3.66\log s - 0.94)}. \quad (37)$$

Kim and Suh [57] performed an experimental study on CHF on a one-dimensional downward heating rectangular channels having a narrow gap by changing the orientation of the copper test heater ina pool of saturated water ar atmospheric pressure. The gas sizes of 1, 2, 5 and 10 mm and the surface orientation angles from the downward-facing position (180°) to the vertical position (90°). They have found that the CHF generally decreases as the surface inclination angle increases and the gasp size decreases. They introduced the equivalent heated surface diameter to account for the width effect and a generalized correlation in the near vertical region is proposed based on their data as

$$\frac{q_{CHF}}{\left[\sigma g\sin\theta(\rho_f - \rho_g)/\rho_g^2\right]^{0.25}} = \frac{0.17}{1 + 6.8\times10^{-4}(\rho_f/\rho_g)^{0.62}(D_{eq}/s)}. \quad (38)$$

Misale et al. [58] performed experimental study of pool boiling CHF with HFE-7100 in inclined narrow spaces by a face-to-face parallel unheated surface, by changing both orientation and gap between the surfaces. The channel gaps are 0.5, 1, 2, 3.5, 5, 10, and 20 mm. The surface orientations investigated are 0° (horizontal upward surface), 45°, 90°, and 135°. They have found that for a fixed channel width, the CHF strongly depends on the channel orientation, assuming a maximum value for near-vertical channels with up-facing heated surface. They proposed a new empirical correlation which takes into account of the channel gas effects for horizontal confined surfaces.

$$q_{CHF} = 0.185 \frac{1}{1 + 71.43e^{-1.32s}} \rho_g^{0.5} h_{fg}[\sigma g(\rho_f - \rho_g)]^{0.25}. \quad (39)$$

Geisler and Bar-Cohen [59] performed experimental studies on CHF for vertical, rectangular parallel-pate channels immersed in FC-72 at atmospheric pressire to elucidate the effects of geometrical confinement in immersion cooled electronics applications. They found that the relative effects of confinement on CHF is independent of surface material and finish and the deterioration in CHF is strongly dependent on channel aspect ratio. They also found that the Bonjour and Lallemand [60] correlation for asymmetrically heated channel accurately predicted their data. They modified this correlation for symmetric channels with spacing-based correction, yielding good agreement with their data, particularly at smaller channel spacings where confinement effects are most significant. The modified correlaton can be found in [59].

Obviously, the studies on confined nucleate pool boiling CHF are very limited. So far there is no generalized prediction method for a wide range of test conditions and fluids. Furthermore, no study connecting confined pool boiling CHF and flow boiling CHF in microscale channels is available but there might be some connections which may help to understand the CHF mechanisms.

CONCLUSIONS

A comprehensive literature review on the CHF of flow boiling (subcoolied and saturated) and pool boiling in micrscale channels and confined spaces is presented in this paper. So far, limited studies on CHF in microscale channels and confined spaces are available in the literature. Especially, there are numerous discrepancies in the existing studies on CHF results and mechanisms. There are no generalized prediction methods for CHF in microscale channels and confined spaces. Based on this review, future work should emphasize the following aspects:

(1) Experimental studies can be undertaken to obtain more data with different fluids and operating conditions to cover the entire range of qualities from the subcooled to the saturated region to get a clearer picture of CHF behavior with critical quality.

(2) More CHF data in both the subcooled and saturated regions are needed for various fluids under a wide range of test conditions to validate the available correlations in the literature.

(3) Further efforts should be made to understand the physical mechanisms of CHF for both subcooled and saturated flow boiling CHFs.

(4) More experimental and theoretical research is needed to understand confined nucleate pool boiling CHF phenomena.

(5) Generalized CHF prediction methods for flow boiling in microchannels and nucleate pool boiling in confined spaces are needed.

(6) Connections of flow boiling in microscale channels and nucleate pool boiling in confined spaces might be helpful in understanding the CHF phenomena.

(7) It is necessary to understand the impact of flow oscillations on the critical heat flux condition.

(8) New research is necessary to investigate the CHF of nanofluids in microscale channels and confined spaces, including experimental and theoretical aspects.

REFERENCES

1. Kandlikar, S.G., *Exp. Therm. Fluid Sci*., 2002, vol. 26, p. 389.
2. Kandlikar, S.G., *Heat Transf., Eng., 2005, vol. 26, p. 5.*
3. Cheng, L. and Mewes, D., *Int. J. Multiphase Flow*, 2006, vol. 32, p. 183.
4. Cheng, L., Ribatski, G., and Thome, J.R., *ASME Appl. Mech. Rev*., 2008, vol. 61, 050802-1-050802-28.
5. Cheng, L., Ribatski, G., and Thome, J.R., *Int. J. Refrig*., 2008, vol. 31, p. 1301.
6. Thome, J.R., *Int. J. Heat Fluid Flow*, 2004, vol. 25, p. 128.
7. Thome, J.R., *Heat Transf. Eng.,* 2006, vol. 27, p. 4.
8. Cheng, L. and Thome, J.R., *Appl. Therm. Eng*., 2009, vol. 29, p. 2426.
9. Cheng, L., Mewes, D., and Luke, A., *Int. J. Heat Mass Transf*., 2007, vol. 50, p. 2744.
10. Cheng, L., E.P. Bandarra Filho, and Thome, J.R., *J. Nanosci. Nanotech*., 2008, vol. 8, p. 3315.
11. Cheng, L., *Recent Pat. Eng.,* 2009, vol. 3, p. 1.
12. Lee, J. and Mudawar, I., *Int. J. Heat Mass Transf*., 2009, vol. 52, p. 3341.
13. Celata, G.P., Cumo, M., and Mariani, A., *Int. J. Heat Mass Transf*., 1993, vol. 36, p. 1269.
14. Celata, G.P., Cumo, M., Mariani, A., Nariai, H., and Inasaka, F., *Int. J. Heat Mass Transf*., 1993, vol. 36, p. 3407.

15. Celata, G.P., Cumo, M., Mariani, A., Simoncini, M., and Zummo, G., *J. Heat Mass Transf*., 1994, vol. 37, p. 347.
16. Celata, G.P., Cumo, M., and Mariani, A., *Int. J. Heat Mass Transf*., 1996, vol. 39, p. 1755.
17. Mudawar, I. and Bowers, M.B., *Int. J. Heat Mass Transf*., 1999, vol. 42, p. 1405.
18. Hall, D.D. and Mudawar, I., *Int. J. Heat Mass Transf*., 1999, vol. 42, p. 1429.
19. Hall, D.D. and Mudawar, I., *Int. J. Heat Mass Transf*., 2000, vol. 43, p. 2573.
20. Hall, D.D. and Mudawar, I., *Int. J. Heat Mass Transf*., 2000, vol. 43, p. 2605.
21. Liu, W., Nariai, H., and Inasaka, F., *Int. J. Heat Mass Transf*., 2000, vol. 43, p. 3371.
22. Kureta, M. and Akimoto, H., *Int. J. Heat Mass Transf*., 2002, vol. 45, p. 4107.
23. Sarma, P.K., Srinivas, V., Sharma, K.V., Dharma Rao, V., and Celata, G.P., *Int. J. Heat Mass Transf*., 2006, vol. 49, p. 42.
24. Zhang, H. Mudawar, I., and Hasan, M.M., *Int. Commun. Heat Mass Transf*., 2007, vol. 34, p. 653.
25. Roday, A.P., Borca-Tasciuc, T., and Jensen, M.K., *J. Heat Transf*., 2008, vol. 130, 012901-1-012901-10.
26. Roday, A.P. and Jensen, M.K., *Int. J. Heat Mass Transf*., 2009, vol. 52, p. 3225.
27. Roday, A.P. and Jensen, M.K., *Int. J. Heat Mass Transf*., 2009, vol. 52, p. 3250.
28. Bergles, A.E. and Kandlikar, S.G., *ASME J. Heat Transf*., 2005, vol. 127, p. 101.
29. Katto, Y. and Ohno, H., *Int. J. Heat and Mass Transf*., 1984, vol. 27, p. 1641.
30. Lazarek, G.M. and Black, G.M., *Int. J. Heat Mass Transf*., 1982, vol. 25, p. 945.
31. Oh, C.H. and Englert, S.B., *Int. J. Heat Mass Transf*., 1993, vol. 36, p. 325.
32. Bowers, M.B. and Mudawar, I., *Int. J. Heat Mass Transf*., 1994, vol. 37, p. 321.
33. Jiang, L., Wong, M., and Zohar, Y., *J. Micro-electromech. Syst.,* 1999, vol. 8, no. 4, p. 358.
34. Qu, W. and Mudawar, I., *Int. J. Heat and Mass Transf*., 2004, vol. 47, p. 2045.
35. Wojtan, L., Revellin, R., and Thome, J.R., *Exp. Therm. Fluid Sci*., 2006, vol. 30, p. 765.
36. Zhang, W., Hibiki, T., Mishima, K., and Mi, Y., *Int. J. Heat Mass Transf*., 2006, vol. 49, p. 1058.
37. Qi, S.L., Zhang, P., Wang, R.Z., and Xu, L.X., *Int. J. Heat Mass Transf*., 2007, vol. 50, p. 5017.
38. Wright, C.T., O'Brien, J.E., and Spall, R.E., *Int. J. Heat Mass Transf*., 2008, vol. 51, p. 1071.
39. Tanaka, F., Hibiki, T., and Mishima, K., *J. Heat Transf*., 2009, vol. 131, 121003-1-121003-7.
40. Kosar, A. and Peles, Y., *J. Heat Transf*., 2007, vol. 129, p. 844.
41. Kuo, C.J. and Peles, Y., *J. Heat Transf*., 2008, vol. 130, 072403-1-072403-7.
42. Wu, Y.W., Su, G.H., Qiu, S.Z., and Hu, B.X., *Int. J. Multiphase Flow* , 2009, vol. 35, p. 977.
43. Revellin, R. and Thome, J.R., *Int. J. Heat Mass Transf*., 2008, vol. 51, p. 1216.

43a. Agostini, B., Revellin, R., Thome, J.R., Fabbri, M., Michel, B., Calmi, D., and Kloter, U., *Int. J. Heat Mass Transf*., 2008, vol. 51, p. 5426.

44. Park, J.E. and Thome, J.R., *Int. J. Heat Mass Transf*., 2010, vol. 53, p. 110.
45. Muaro, A.W., Thome, J.R., Toto, D., and Vanoli, G.P., *Exp. Therm. Fluid. Sci*., 2010, vol. 34, p. 81.
46. Kosar, A., *Int. J. Thermal Sci*., 2009, vol. 48 p. 261.
47. Patankar, U. and Puranik, B., *Proc. Fourth Int. Conf. on Nanochannels, Microchannels, and Minichannels,* Rochester, New York, 2003, ICMM2003-1016.
48. Roach, G.M. Jr., Abdel_Khalik, S.I., Ghiaasiaan, S.M., Dowling, M.F., and Jeter, S.M., *Nucl. Sci. Eng.,* 1999, vol. 131, p. 411.
49. Bergles, A.E. and Rohsenow, W.M., *Forced-Convection Surface-Boiling Heat Transf., and Burnout in Tubes of Small Diameter*, Contract AF 19(604)-7355 Report, Department of Mechanical Engineering, Massachusetts Institute of Technology, 1962.
50. Yu, W., France, D.M., Wambsganss, M.W., and Hull, J.R., *Int. J. Multiphase Flow* , 2002, vol. 28, p. 927.
51. Katto, Y. and Kosho, Y., *Int. J. Multiphase Flow* , 1979, vol. 5, p. 219.
52. Monde, M., Kusuda, H., and Uehara, H., *ASME J. Heat Transf*., 1982, vol. 104, p. 300.
53. Fujita, Y., Ohta, H., and Uchida, S., *Int. J. Heat Mass Transf*., 1988, vol. 31, p. 229.
54. Kim, S.H., Baek, W.P., and Chang, S.H., *Nucl. Eng. Design*, 2000, vol. 199, p. 41.
55. Chyu, M.C., *Int. J. Heat Mass Transf*., 1988, vol. 31, p. 1993.
56. Kim, Y.H. and Suh, K.Y., *Nucl. Eng. Design*, 2003, vol. 226, p. 277.
57. Miscale, M., Gugliemini, G., and Priarone, A., *Int. J. Refrig*., 2009, vol. 32, p. 235.
58. Geisler, K.J.L. and Bar-Cohen, A., *Int. J. Heat Mass Transf*., 2009, vol. 52, p. 2427.
59. Bonjour J. and Lallemand, M., *Int. Commun. Heat Mass Transf*., 1997, vol. 24, no. 2, p. 191.
60. Kuan, W.K. and Kandlikar, S.G., *J. Heat Transf*., 2008, vol. 130, 034503-1-034503-5.